数理解析研究所講究録 1265 巻 2002 年 173-183

A Numerical Approximation Method for a Non-local Operator Applied to Radiation Problem

Haniffa M. NASIR (ハニファ モハメド ナシル), University of Peradeniya [1)]

KAKO, Takashi (加古 孝), The University of Electro-Communications (電気通信大学) [2)]

Abstract: In the finite element approximation of the exterior Helmholtz problem, we propose an approximation method to implement the DtN mapping formulated as a pseudo-differential operator on a computational artificial boundary. The method is then combined with the fictitious domain method. Our method directly gives an approximation matrix for the sesqui-linear form for the DtN mapping. The eigenvalues of the approximation matrix is simplified to a closed form and can be computed efficiently by using a continued fraction formula. Solution outside the computational domain and the far-field solution can also be computed efficiently by expressing them as operations of pseudo-differential operators. An inner artificial DtN boundary condition is also implemented by our method. We prove the convergence of the solution of our method and compare the performance with the standard finite element approximation based on the Fourier series expansion of the DtN operator. The efficiency of our method is demonstrated through numerical examples.

1 Introduction

We consider the following two-dimensional exterior Helmholtz problem:

$$
\begin{aligned}
-\Delta u - k^2 u &= 0 && \text{in } \Omega = \mathbb{R}^2 \backslash O, && \text{(1a)}\\
\frac{\partial u}{\partial n} &= -\frac{\partial u^{\mathrm{inc}}}{\partial n} && \text{on } \partial\Omega, && \text{(1b)}\\
\lim_{r\to\infty} \sqrt{r}\left(\frac{\partial u}{\partial r} - \mathrm{i}ku\right) &= 0, && && \text{(1c)}
\end{aligned}
$$

where Ω is the interior of the complement of a bounded region O in $\mathbb{R}^2$ with smooth boundary $\partial\Omega$ on which the Neumann boundary condition (1b) is imposed and (1c) is the Sommerfeld radiation condition at infinity.

The equation can be used to simulate the scattering phenomena of time-harmonic electromagnetic or acoustic wave by an obstacle O which is sometimes called a scatterer. Here, $u^{\mathrm{inc}}(\mathbf{x}) = \mathrm{e}^{\mathrm{i}\mathbf{k}.\mathbf{x}}$ is the time-harmonic incident plane wave whose direction of propagation is given by the vector $\mathbf{k}$, and $\mathbf{n}$ is the outward unit normal on the scatterer (see Fig. 1).

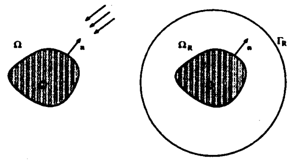

Figure 1: Obstacle and artificial boundary

In order to solve the exterior Helmholtz problems numerically, it is a common practice to introduce an artificial boundary to limit the area of computation and to prescribe an artificial boundary condition on this boundary. The boundary condition is expected to "absorb" the outgoing waves and to exclude any incoming waves. Various artificial boundary conditions have been proposed in the literature for this purpose (see Givoli [6], Ihlenburg [8] and the references therein). The artificial boundary condition that gives the solution to (1) is given by the Dirichlet to Neumann (DtN) mapping.

[1]University of Peradeniya, Sri Lanka. Email: nasirhm@fedu.uec.ac.jp
[2]The University of Electro-Communications, Chofu, Japan. Email: kako@im.uec.ac.jp

In the finite element approximation of the problem, the implementation of the DtN mapping or its approximations has been a subject of interest by many authors (see, for example, Kako [9], Liu [13], Liu and Kako [14] and the references therein). As for the case of using the exact DtN mapping, MacCamy and Marin [16] used an integral representation of the DtN mapping and obtain its finite element matrix by explicitly solving some auxiliary integral equations. Keller and Givoli [10] used the Fourier series representation of the DtN mapping and use the standard finite element technique to obtain the matrix in an infinite series form (see also Ernst [4] and Heikkola et al. [7]).

In this paper, we propose an approximation method to implement the DtN mapping by expressing it in a form of pseudo-differential operator. The finite element approximation corresponding to the sesqui-linear form of the pseudo-differential operator is given by a matrix which we call a mixed type approximation matrix. This matrix is obtained by replacing the argument of the function in the pseudo-differential operator, which in this case is the Laplacian on the unit circle, by its finite element matrix. This gives a matrix in a closed form which can be efficiently computed by a continued fraction without use of the Hankel function and its derivative. The computational cost for the boundary condition in this method is $O(n_\theta)$ where n_θ is the number of partitions in angular direction.

When the origin of the polar-coordinate system is outside the obstacle domain, one can consider an inner artificial boundary that excludes the origin from the computational domain and another DtN boundary condition is imposed on the inner artificial boundary which is also treated by our method.

The solution outside the computational domain and the far-field pattern are expressed in closed forms by using pseudo-differential operators and our previous method can also be applied to compute the quantities.

We consider the fictitious domain method to form the linear equations and use the Krylov subspace iterative method to solve the linear system (Kuznetsov et al. [12], Heikkola et al. [7]).

The rest of the paper is organized as follows. In Section 2, we review the artificial boundary condition and its standard finite element approximation. In Section 3, we introduce a mixed type method for the artificial boundary and its application in fictitious domain method. In Section 4, we consider the application of the mixed type method for the solution outside the computational domain and the far-field pattern. In Section 5, we prove the convergence of the solutions. We present the results of numerical tests in Section 6 and make some concluding remarks in Section 7.

2 Artificial boundaries and artificial boundary conditions

For the numerical treatment of the problem (1), the unbounded domain Ω is truncated by an artificial boundary, denoted by Γ_R, and an artificial boundary condition is introduced. The artificial boundary is a circle of radius R and we denote by B_R the circular domain of radius R bounded by Γ_R. The approximate boundary value problem is then given by

$$-\Delta u - k^2 u = 0 \qquad \text{in } \Omega_R \equiv \Omega \cap B_R, \tag{2a}$$

$$\frac{\partial u}{\partial n} = -\frac{\partial u^{\text{inc}}}{\partial n} \qquad \text{on } \partial\Omega, \tag{2b}$$

$$\frac{\partial u}{\partial r} = -Mu \qquad \text{on } \Gamma_R, \tag{2c}$$

where M is the DtN mapping which we regard as a pseudo-differential operator as a function of the Laplacian operator $D^2 := -\partial^2/\partial\theta^2$ and is given by

$$M(D^2)u(R,\theta) \equiv -\frac{k}{2\pi}\sum_{n=-\infty}^{\infty}\frac{H^{(1)'}(kR;n)}{H^{(1)}(kR;n)}\int_0^{2\pi} u(R,\phi)e^{in(\theta-\phi)}d\phi \tag{3}$$

$$= -k\frac{H^{(1)'}(kR;\sqrt{D^2})}{H^{(1)}(kR;\sqrt{D^2})}u(R,\theta), \tag{4}$$

where we denote by $H^{(1)}(x;\nu)$ the Hankel function of the first kind of order ν. The basic definition of pseudo-differential operator can be found, for example, in Nirenberg [18] and Taylor [19].

2.1 Weak formulation and FEM

Let $V \equiv H^1(\Omega_R)$ where $H^s(\Omega_R)$ is the Sobolev space of order $s \in \mathbb{R}$ in Ω_R and $\gamma : H^1(\Omega_R) \to H^{1/2}(\Gamma_R)$ be the trace operator. Then, the weak formulation of the boundary value problem (2) is: Find $u \in V$ such that

$$a(u,v) + \langle \gamma u, \gamma v\rangle_M = (\partial u^{\mathrm{inc}}/\partial n, v)_{\partial\Omega} \qquad \forall v \in V, \tag{5}$$

where the sesqui-linear forms $a(\cdot,\cdot)$, $\langle\cdot,\cdot\rangle_M$ and $(\cdot,\cdot)_{\partial\Omega}$ respectively are

$$\begin{aligned} a(u,v) &= \int_{\Omega_R} \left(\frac{\partial u}{\partial r}\frac{\partial \bar v}{\partial r} + \frac{1}{r^2}\frac{\partial u}{\partial \theta}\frac{\partial \bar v}{\partial \theta} - k^2 u\bar v\right) r dr d\theta, \quad u,v \in H^1(\Omega_R), \\ \langle p,q\rangle_M &= \int_0^{2\pi} (Mp)(\theta)\bar q(\theta)\, R d\theta, \qquad p,q \in H^{1/2}(\Gamma_R), \\ \text{and } (f,g)_{\partial\Omega} &= \int_{\partial\Omega} f\bar g d\sigma, \quad f,g \in L^2(\partial\Omega). \end{aligned}$$

Now, based on the element partitioning of the computational domain described in Subsection 3.2, we form a finite dimensional subspace V_h of V. The finite element approximate problem is then given by: Find $u_h \in V_h$ such that

$$a(u_h,v_h) + \langle \gamma u_h, \gamma v_h\rangle_M = (\partial u^{\mathrm{inc}}/\partial n, v_h)_{\partial\Omega}, \qquad \forall v_h \in V_h. \tag{6}$$

2.2 FEM matrix of DtN mapping by the Fourier mode representation

The finite element approximation matrix corresponding to the DtN mappings given in the form of (3) has been obtained by several authors (e.g., Ernst [4]).

According to the finite element partitioning of Ω_R, the artificial boundary Γ_R is discretized by a uniform partitioning with n_θ nodes and an equal number of intervals. We use piecewise linear continuous functions $\{\phi_i\}_{i=0}^{n_\theta-1}$ as the basis for the finite element approximation. The sesqui-linear form corresponding to the DtN mapping is represented in terms of the Fourier modes as

$$\langle \gamma u_h, \gamma v_h\rangle_M = \sum_{n=-\infty}^{\infty} RM(n^2)\widehat{\gamma u}_{h,n}\overline{\widehat{\gamma v}_{h,n}} \tag{7}$$

where $\hat p_{h,n}$ is the Fourier coefficient of p_h given by $\hat p_{h,n} = \frac{1}{\sqrt{2\pi}}\int_0^{2\pi} p_h(\phi)\mathrm{e}^{-\mathrm{i}n\phi}d\phi$.

We express $p_h = \sum_{j=0}^{n_\theta-1}\tilde p_{h,j}\phi_j(\theta)$ and set $[\tilde p_h] := [\tilde p_{h,0}, \tilde p_{h,1}, \cdots, \tilde p_{h,n_\theta-1}]^T$. By performing the integration, we get $\widehat{\gamma u}_{h,n} = \mu_n Q_{h,n}[\widetilde{\gamma u}_h]$, where $\mu_0 = \sqrt{h_\theta}$, $\mu_n = 2(1-\cos nh_\theta)/(n^2 h_\theta^{3/2})$ for $n \neq 0$, $Q_{h,n} = [1, \mathrm{e}^{\mathrm{i}2\pi n/n_\theta}, \cdots, \mathrm{e}^{\mathrm{i}2\pi n(n_\theta-1)/n_\theta}]/\sqrt{n_\theta}$ and $h_\theta = 2\pi/n_\theta$. Clearly, $Q_{h,j} = Q_{h,ln_\theta+j}$ for $0 \le j < n_\theta, l \in \mathbb{Z}$. Substituting $\widehat{\gamma u}_{h,n}$ and $\widehat{\gamma v}_{h,n}$ in (7), we have

$$\begin{aligned} \langle \gamma u_h, \gamma v_h\rangle_M &= \sum_{n=-\infty}^{\infty} \overline{[\widetilde{\gamma v}_h]^T Q_{h,n}^T} RM(n^2)\mu_n^2 Q_{h,n}[\widetilde{\gamma u}_h] \\ &= \sum_{j=0}^{n_\theta-1} \overline{[\widetilde{\gamma v}_h]^T Q_{h,j}^T} \sum_{l=-\infty}^{\infty} RM((ln_\theta+j)^2)\mu_{ln_\theta+j}^2 Q_{h,j}[\widetilde{\gamma u}_h] \\ &=: (\mathbf{M}_h^{\mathrm{std}}[\widetilde{\gamma u}_h], [\widetilde{\gamma v}_h])_{\mathbb{C}^{n_\theta}}, \end{aligned} \tag{8}$$

where $\mathbf{M}_h^{\mathrm{std}} = Q_h^*\Lambda_h^{\mathrm{std}}Q_h$; Q_h is the unitary matrix formed by the rows $Q_{h,j}, 0 \le j < n_\theta$, and Λ_h^{std} is a diagonal matrix whose jth diagonal element is the eigenvalue of $\mathbf{M}_h^{\mathrm{std}}$ and is given by

$$\lambda_{h,j}^{\mathrm{std}} = \begin{cases} RM(0)h_\theta, & j = 0, \\ \dfrac{4(1-\cos jh_\theta)^2}{h_\theta^3}\displaystyle\sum_{l=-\infty}^{\infty}\frac{RM((ln_\theta+j)^2)}{(ln_\theta+j)^4}, & j \neq 0. \end{cases}$$

Note that $\lambda_{h,j}^{\mathrm{std}} = \lambda_{h,n_\theta-j}^{\mathrm{std}}$. From the estimate $|M(n^2)| \le C(1+|n|)$ (see Masmoudi [17]), the sum tends to $RM(j^2)/j^4$ and $4(1-\cos jh_\theta)^2/h_\theta^4 \to j^4$ as $h_\theta \to 0$. Thus, we get the following facts for $0 \le j < n_\theta/2$:

$$\begin{aligned} \lambda_{h,j}^{\mathrm{std}}/h_\theta &\to RM(j^2) \text{ as } h_\theta \to 0, & (9)\\ |\lambda_{h,j}^{\mathrm{std}}| &\le Ch_\theta(1+|j|). & (10) \end{aligned}$$

3 A mixed type method

We propose a method which gives an approximation matrix directly for the sesqui-linear form $\langle \gamma u, \gamma v\rangle_M$. The matrix is circulant and its eigenvalues are one term expression which can be computed efficiently by means of a continued fraction (see Section 3.1). The standard finite element matrix $\mathbf{M}_h^{\mathrm{std}}$ is then replaced by this matrix in the linear equations to be solved.

With the same partition and basis functions considered in the last section, the finite element matrices corresponding to the sesqui-linear forms $(u', v')_{L^2(0,2\pi)}$ and $(u,v)_{L^2(0,2\pi)}$ respectively are given by

$$[A]_h = \frac{1}{h_\theta}\mathrm{Circ}(-1,2,-1), \qquad [B]_h = \frac{h_\theta}{6}\mathrm{Circ}(1,4,1), \tag{11}$$

where we denote by $\mathrm{Circ}(a,b,c)$ the circulant matrix for which the main diagonal is formed by b and the lower and upper diagonals are formed by a and c respectively.

Definition 1. A mixed type approximation matrix corresponding to the operator $M(D^2)$ is defined by

$$\mathbf{M}_h^{\mathrm{mixed}} := [B]_h RM([B]_h^{-1}[A]_h), \tag{12}$$

where the matrices $[A]_h$ and $[B]_h$ are given in (11).

In the error analysis, we introduce a sesqui-linear form (15) corresponding to this matrix. Since $\mathbf{M}_h^{\mathrm{mixed}}$ is circulant, it can be expressed as $\mathbf{M}_h^{\mathrm{mixed}} = Q^*\Lambda_h^{\mathrm{mixed}}Q$ as in the standard FEM case. The jth eigenvalue of $\mathbf{M}_h^{\mathrm{mixed}}$ is given by $\lambda_{h,j}^{\mathrm{mixed}} = RM(\nu_{h,j}^2)\lambda_{h,j}^{[B]_h}$ where $\nu_{h,j}^2 = \lambda_{h,j}^{[A]_h}/\lambda_{h,j}^{[B]_h}$; $\lambda_{h,j}^{[A]_h} = 2(1-\cos jh_\theta)/h_\theta$ and $\lambda_{h,j}^{[B]_h} = h_\theta(2+\cos jh_\theta)/3$. Clearly, we have $\lambda_{h,j}^{\mathrm{mixed}} = \lambda_{h,n_\theta-j}^{\mathrm{mixed}}$ and the similar estimates to (9) and (10) hold for $\lambda_{h,j}^{\mathrm{mixed}}$ as well as $\lambda_{h,j}^{\mathrm{std}}$.

3.1 Continued fraction

In this subsection, we present an efficient computation of the logarithmic derivatives of the Bessel and Hankel functions which appear in the DtN mappings. The key idea is to use continued fraction forms for the logarithmic derivatives. These continued fractions are rapidly converging and an efficient algorithm for computing them is readily available as the modified Lentz's method (Thompson and Barnett [20]). The continued fraction for the DtN mapping on the exterior artificial boundary is given by

$$x\frac{H^{(1)\,\prime}(x;\nu)}{H^{(1)}(x;\nu)} = \mathrm{i}x - \frac{1}{2} + \mathrm{i}\frac{(1/2)^2-\nu^2}{2(x+\mathrm{i})+}\,\frac{(3/2)^2-\nu^2}{2(x+2\mathrm{i})+\cdots},$$

where $x = kR$, and the continued fraction for the DtN mapping on the inner artificial boundary is given by

$$x\frac{J'(x;\nu)}{J(x;\nu)} = \nu - \frac{x}{2(\nu+1)/x-}\,\frac{1}{2(\nu+2)/x-\cdots},$$

where $x = kr_0$.

These continued fractions converges for all values of ν and x except those in the neighborhood of zero. It converges very rapidly for $x \ge \sqrt{\nu(\nu+1)}$.

3.2 Fictitious domain method

In order to solve the problem with general obstacle, we use the fictitious domain method [4, 7] to form the approximation subspace V_h. For this, the computational domain Ω_R is extended to a fictitious domain Ω_R^F which is a circular annulus and includes the obstacle boundary. When the obstacle is not narrow and contains a larger neighborhood of the origin, Ω_R is extended inside the obstacle to form the fictitious domain. When the obstacle is thin, we choose the polar coordinate system such that the origin is outside of the obstacle and Ω_R^F is obtained as the union of Ω_R and the obstacle domain O (see Fig. 2).

Now, the annulus fictitious domain is partitioned by an orthogonal polar mesh. The nodes of the mesh next to the boundary of the obstacle O are shifted onto the boundary $\partial\Omega$, and the modified quadrilateral elements in the computational domain are triangulated such that the resulting mesh gives a shape regular triangulation (Börgers [1]). This leads to a locally fitted mesh, which is topologically equivalent to the original mesh and differs from it only in an h-neighborhood of the obstacle boundary. The mesh inside the obstacle domain is discarded to obtain the mesh for Ω_R.

The approximation subspace V_h consists of functions u_h such that the restrictions of u_h in the unmodified rectangles are bilinear and the restrictions on the triangles near the obstacle boundary are linear.

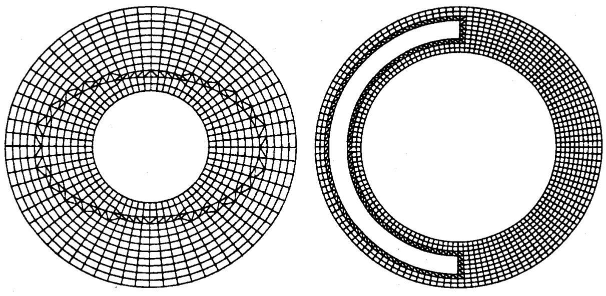

Figure 2: : Fictitious domains and locally fitted mesh

For more details on the fictitious domain method, see Kuznetsov and Lipnikov[12] and Heikkola[7].

4 Further applications

The mixed type method can be used in other cases of radiation problems where pseudo-differential operators appear. We consider cases of an inner artificial boundary, computing solution outside the computational domain and computing the far field pattern.

4.1 Inner artificial boundary

When the obstacle does not contain the origin, one can introduce an inner artificial boundary Γ_{r_0} which is a circle of radius r_0. Then we consider the computational domain Ω_R which also excludes the disc of radius r_0 and we impose an inner DtN boundary condition on Γ_{r_0} given by

$$\frac{\partial u}{\partial r} = Nu = k\frac{J'(kr_0;\sqrt{D^2})}{J(kr_0;\sqrt{D^2})}u(r_0,\theta) \qquad \text{on } \Gamma_{r_0},$$

where $J(x;\nu)$ is the Bessel function of order ν. Its corresponding sesqui-linear form $\langle\gamma_0 u, \gamma_0 v\rangle_N$ will be added to the weak form (5). In the finite element approximation, we replace its standard FEM matrix by the mixed type matrix $\mathrm{N}_h^{\mathrm{mixed}}$ defined analogous to Definition 1.

4.2 Solution outside the computational domain and far field pattern

The solution on a circle of radius r outside the computational domain can be represented by series with respect to the solutions on the artificial boundary. For the exterior region, the solution $p_r(\theta) = u(r,\theta)$ can be expressed as a pseudo-differential operator form as follows:

$$p_r(\theta) = S_1(D^2)u = \frac{H(kr;\sqrt{D^2})}{H(kR;\sqrt{D^2})}p_R(\theta), \quad r \geq R, \tag{13}$$

and for the interior region the solution is given by

$$p_r(\theta) = S_2(D^2)u = \frac{J(kr;\sqrt{D^2})}{J(kr_0;\sqrt{D^2})}p_{r_0}(\theta), \quad r \leq r_0.$$

The far-field pattern corresponding to the solution is obtained by using the asymptotic formula of the Hankel function in the solution (13) and is given by

$$F(D^2)u = \sqrt{\frac{2}{\pi k}}\frac{\mathrm{e}^{-i\pi/2(\sqrt{D^2}+1/2)}}{H^{(1)}(kR;\sqrt{D^2})}p_R(\theta).$$

In order to compute these solutions, one can use the finite element method in which we apply the mixed type method. The weak formulation of the generic form $p_r(\theta) = S(D^2)p_0(\theta)$ is given by $(p_r, q) = \langle p_0, q\rangle_S$ and hence, using the uniform partition as before, and using finite element method, we get the matrix equation

$$[B]_h P_r = \mathbf{S}_h^{\text{mixed}} P_0, \tag{14}$$

where the matrix $\mathbf{S}_h^{\text{mixed}}$ is given as in (12) for the function S and P_r and P_0 are column vectors corresponding to $p_r(\theta)$ and $p_0(\theta)$ respectively with respect to the nodal basis functions. One can cancel the pre-multiplication of the matrix $[B]_h$ on both sides of (14). Hence, computing the solution is reduced to a matrix multiplication which can be performed efficiently by using FFT. Clearly, the solution at radius r is not coupled with solutions of the adjacent circles. Hence, in order to save computing time, one can choose the minimum amount of circles for the solution that will provide the resolution of the waves. As a rule of thumb, one can choose 10 radial intervals per wavelength.

5 Convergence Analysis

Let $a_0(u,v) = \int_{\Omega_R}(\nabla u\cdot\overline{\nabla v}+u\bar{v})dx$ and $b_0(u,v) = \int_{\Omega_R} -(k^2+1)u\bar{v}dx$ and let $P_h^{\Gamma_R} : H^1(\Gamma_R) \longrightarrow V_h^{\Gamma_R}$ be the orthogonal projection with respect to $H^1(\Gamma_R)$-inner product where $V_h^{\Gamma_R} = \{\gamma v_h : v_h \in V_h\}$. We define a sesqui-linear form on $H^1(\Gamma_R)$ corresponding to the mixed type method as

$$\langle p,q\rangle_{M,h}^{\text{mixed}} = (\mathbf{M}_h^{\text{mixed}}[\widetilde{P_h^{\Gamma_R}p}], [\widetilde{P_h^{\Gamma_R}q}])_{\mathbb{C}^{n_\theta}}, \qquad p,q \in H^1(\Gamma_R). \tag{15}$$

With $a_M^{\text{std}}(u,v) := a_0(u,v) + b_0(u,v) + \langle\gamma u, \gamma v\rangle_M$ and $a_{M,h}^{\text{mixed}}(u_h,v_h) := a_0(u_h,v_h) + b_0(u_h,v_h) + \langle\gamma u_h, \gamma v_h\rangle_{M,h}^{\text{mixed}}$, we have the following problems:

$$(E): \qquad a_M^{\text{std}}(u,v) = \langle f,v\rangle, \qquad \forall v \in V;$$
$$(E)_h^{\text{mixed}}: \qquad a_{M,h}^{\text{mixed}}(u_h,v_h) = \langle f,v_h\rangle, \qquad \forall v_h \in V_h,$$

where $\langle f,v\rangle = (\partial u^{\text{inc}}/\partial r, v)_{\partial\Omega}$. In the following, we denote by $\|\cdot\|_{s,\Omega}$, $s \in \mathbb{R}$ the norm on the Sobolev space $H^s(\Omega), \Omega = \Omega_R$ or Γ_R (Ciarlet and Lion [3]).

Theorem 1. *Let $u \in V$ be the solution of (E). Then, there exists h_0 such that for all $h \in (0,h_0)$, there exist unique solutions $u_h \in V_h$ of $(E)_h^{\text{mixed}}$ such that*

$$\lim_{h\to 0} \|u - u_h\|_{1,\Omega_R} = 0.$$

To prove the theorem, we need some lemmas. Let u and u_h be the solutions of (E) and $(E)_h^{\text{mixed}}$ respectively, and put $e_h = u - u_h$. Since $\partial\Omega$ is smooth, $u \in H^2(\Omega_R)$. Equating (E) and $(E)_h^{\text{mixed}}$ and adding and subtracting $\langle \gamma u, \gamma v_h\rangle_{M,h}^{\text{mixed}}$, we have,

$$a_0(e_h, v_h) + b_0(e_h, v_h) + \langle \gamma e_h, \gamma v_h\rangle_{M,h}^{\text{mixed}} + r_h(u, v_h) = 0, \tag{16}$$

where $r_h(u,v) = \langle \gamma u, \gamma v\rangle_M - \langle \gamma u, \gamma v\rangle_{M,h}^{\text{mixed}}$. Now we have the following lemmas.

Lemma 1. *There exists a constant $C_1(h)$ with $\lim_{h\to 0} C_1(h) = 0$ and h_0 such that for all $h \in (0, h_0)$,*

$$|r_h(u, v_h)| \le C_1(h)\|u\|_{2,\Omega_R}\|v_h\|_{1,\Omega_R}, \text{ for all } v_h \in V_h.$$

Lemma 2. *For every $\varepsilon > 0$, there exists a constant $C_2(\varepsilon, h)$ with $\lim_{h\to 0} C_2(\varepsilon, h) = 0$ such that*

$$|a_{M,h}^{\text{mixed}}(e_h, e_h)| \le \varepsilon\|e_h\|_{1,\Omega_R}^2 + C_2(\varepsilon, h)\|u\|_{2,\Omega_R}^2.$$

Lemma 3. *There exist two constants $C_3(h)$ and $C_4(h)$ with $\lim_{h\to 0} C_3(h) = \lim_{h\to 0} C_4(h) = 0$ such that*

$$|b_0(e_h, e_h)| \le C_3(h)\|e_h\|_{1,\Omega_R}^2 + C_4(h)\|u\|_{2,\Omega_R}^2.$$

Proof. Proof of Theorem 1

Since $\operatorname{Re} M(\nu^2) > 0$ for all $\nu \in \mathbb{R}$ (Koyama [11]), we have $\operatorname{Re}\langle \gamma e_h, \gamma e_h\rangle_{M,h}^{\text{mixed}} \ge 0$.

Considering the real part of $\|e_h\|_{1,\Omega_R}^2 = a_0(e_h, e_h) = a_{M,h}^{\text{mixed}}(e_h, e_h) - b_0(e_h, e_h) - \langle \gamma e_h, \gamma e_h\rangle_{M,h}^{\text{mixed}}$ and lemmas 2 and 3, we have

$$\begin{aligned}\|e_h\|_{1,\Omega_R}^2 &\le \operatorname{Re} a_{M,h}^{\text{mixed}}(e_h, e_h) - \operatorname{Re} b_0(e_h, e_h)\\ &\le \varepsilon\|e_h\|_{1,\Omega_R}^2 + C_2(\varepsilon, h)\|u\|_{2,\Omega_R}^2 + C_3(h)\|e_h\|_{1,\Omega_R}^2 + C_4(h)\|u\|_{2,\Omega_R}^2.\end{aligned}$$

Hence, we have $(1 - \varepsilon - C_3(h))\|e_h\|_{1,\Omega_R}^2 \le (C_2(\varepsilon, h) + C_4(h))\|u\|_{2,\Omega_R}^2$. Choosing ε small enough such that $(1 - \varepsilon - C_3(h)) > 1 - 2\varepsilon > 0$, we get $\|e_h\|_{1,\Omega_R}^2 \le (1 - 2\varepsilon)^{-1}(C_2(\varepsilon, h) + C_4(h))\|u\|_{2,\Omega_R}^2 \longrightarrow 0$ as $h \longrightarrow 0$.

For the uniqueness, if $f = 0$, then $u = 0$ by the solvability of (E). Then, by the last inequality, $e_h = -u_h = 0$. □ □

Proof. Proof of Lemma 1 First, we establish an estimate for $\|p_h\|_{s,\Gamma_R}, s \in \mathbb{R}$. Analogous to (7) and (8) (with $M(j^2) = (1 + j^2)^s$ and $R = 1$), we have

$$\begin{aligned}\|p_h\|_{s,\Gamma_R}^2 &= \sum_{j=0}^{n_\theta - 1}\sum_{l=-\infty}^{\infty}(1 + (ln_\theta + j)^2)^s \mu_{ln_\theta + j}^2 |Q_{h,j}[\tilde{p}_h]|^2\\ &\ge \sum_{j=0}^{n_\theta - 1}(1 + j^2)^s \mu_j^2 |Q_{h,j}[\tilde{p}_h]|^2 \ge C\sum_{j=0}^{n_\theta - 1} h_\theta(1 + j^2)^s |Q_{h,j}[\tilde{p}_h]|^2\end{aligned} \tag{17}$$

due to the fact that $\mu_j^2 = h_\theta(\sin(jh_\theta/2)/(jh_\theta/2))^4 \ge Ch_\theta$ for $0 \le j < n_\theta/2$.

We write $r_h(u, v_h) = \langle \gamma u - P_h^{\Gamma_R}\gamma u, \gamma v_h\rangle_M + (\langle P_h^{\Gamma_R}\gamma u, \gamma v_h\rangle_M - \langle \gamma u, \gamma v_h\rangle_{M,h}^{\text{mixed}}) =: (I) + (II)$. From standard estimates: $\|(I - P_h^{\Gamma_R})\gamma u)\|_{m,\Gamma_R} \le Ch_\theta^{1-m}\|\gamma u\|_{1,\Gamma_R}, m = 0, 1$, we get $\|(I - P_h^{\Gamma_R})\gamma u)\|_{\frac{1}{2},\Gamma_R} \le Ch_\theta^{\frac{1}{2}}\|\gamma u\|_{1,\Gamma_R}$ by interpolation.

Since the DtN operator is a bounded operator from $H^{1/2}(\Gamma_R)$ into $H^{-1/2}(\Gamma_R)$ (Masmoudi [17]), we have,

$$|(I)| \le C\|(I - P_h^{\Gamma_R})\gamma u)\|_{\frac{1}{2},\Gamma_R}\|\gamma v_h\|_{\frac{1}{2},\Gamma_R} \le Ch_\theta^{\frac{1}{2}}\|\gamma u\|_{1,\Gamma_R}\|\gamma v_h\|_{\frac{1}{2},\Gamma_R}.$$

For the treatment of (II), we adjust the index range as $-n_\theta/2 \le j \le n_\theta/2$ for simplicity. We have from the estimates (9) and (10) for $\lambda_{h,j}^{\text{std}}$ and $\lambda_{h,j}^{\text{mixed}}$ that for an arbitrarily fixed j_0, there exists $C(j_0,h)$ with $\lim_{h\to 0} C(j_0,h) = 0$ such that $|\lambda_{h,j}^{\text{std}} - \lambda_{h,j}^{\text{mixed}}| \le C(j_0,h)h_\theta$, for all $|j| \le j_0$ and $|\lambda_{h,j}^{\text{std}} - \lambda_{h,j}^{\text{mixed}}| \le Ch_\theta(1+|j|)$, for all $j \ne 0$. Now, denoting $Q_u = |Q_{h,j}[\widetilde{P_h^{\Gamma_R}\gamma u}]|$ and $Q_{v_h} = |Q_{h,j}[\widetilde{\gamma v_h}]|$ for brevity, and using (17), we get

$$
\begin{aligned}
|(II)| &= |((\mathbf{M}_h^{\text{std}} - \mathbf{M}_h^{\text{mixed}})[\widetilde{P_h^{\Gamma_R}\gamma u}], [\widetilde{\gamma v_h}])| \\
&\le \sum_{|j|\le j_0} |\lambda_{h,j}^{\text{std}} - \lambda_{h,j}^{\text{mixed}}| Q_u Q_{v_h} + \sum_{|j|> j_0} |\lambda_{h,j}^{\text{std}} - \lambda_{h,j}^{\text{mixed}}| Q_u Q_{v_h} \\
&\le C(j_0,h) \sum_{|j|\le j_0} h_\theta Q_u Q_{v_h} + C \sum_{|j|>j_0} h_\theta (1+|j|) Q_u Q_{v_h} \\
&\le C(j_0,h) \|P_h^{\Gamma_R}\gamma u\|_{0,\Gamma_R} \|\gamma v_h\|_{0,\Gamma_R} \\
&\quad + C|j_0|^{-\frac{1}{2}} \sum_{|j|>j_0} h_\theta (1+|j^2|)^{\frac{1}{2}} Q_u (1+|j^2|)^{\frac{1}{4}} Q_{v_h} \\
&\le (C(j_0,h) + C|j_0|^{-1/2}) \|\gamma u\|_{1,\Gamma_R} \|\gamma v_h\|_{\frac{1}{2},\Gamma_R}.
\end{aligned}
$$

Hence, adding (I) and (II), we have $|r_h(u,v_h)| \le C_1(h)\|\gamma u\|_{1,\Gamma_R}\|\gamma v_h\|_{\frac{1}{2},\Gamma_R} \le C_1(h)\|u\|_{2,\Omega_R}\|v_h\|_{1,\Omega_R}$ with $C_1(h) = Ch_\theta^{1/2} + C(j_0,h) + C|j_0|^{-1/2}$. For an arbitrary $\varepsilon > 0$, we first choose j_0 such that $|j_0|^{-1/2} < \varepsilon/2$, and then we can see that there exists $h_0 > 0$ such that $Ch_\theta^{1/2} + C(j_0,h) < \varepsilon/2$ for all $0 < h < h_0$. □ □

Proof. Proof of Lemma 2 By (16), we have $a_{M,h}^{\text{mixed}}(e_h,e_h) = a_{M,h}^{\text{mixed}}(e_h, u-u_h) = a_{M,h}^{\text{mixed}}(e_h, u - v_h) + r_h(u, u - v_h - e_h)$, and hence,

$$
\begin{aligned}
|a_{M,h}^{\text{mixed}}(e_h,e_h)| &\le C\|e_h\|_{1,\Omega_R}\|u-v_h\|_{1,\Omega_R} + C_1(h)\|u-v_h-e_h\|_{1,\Omega_R}\|u\|_{2,\Omega_R} \\
&\le (Ch + C_1(h))\|u\|_{2,\Omega_R}\|e_h\|_{1,\Omega_R} + C_1(h)h\|u\|_{2,\Omega_R}^2 \\
&\le \varepsilon/2\|e_h\|_{1,\Omega_R}^2 + C_2(\varepsilon,h)\|u\|_{2,\Omega_R}^2
\end{aligned}
$$

where $C_2(\varepsilon,h) = \frac{1}{2\varepsilon}(Ch + C_1(h))^2 + C_1(h)h \to 0$ as $h \to 0$. □ □

Proof. Proof of Lemma 3 There exists a unique $w \in H^2(\Omega_R)$ such that $a_M^{\text{std}}(v,w) = -(v,(k^2+1)e_h)$ for all $v \in V$, and

$$
\|w\|_{2,\Omega_R} \le C\|e_h\|_{0,\Omega_R}. \tag{18}
$$

where C is a constant independent of e_h and w. Using (16), we have, for all $v_h \in V_h$,

$$
\begin{aligned}
b_0(e_h,e_h) &= a_M^{\text{std}}(e_h,w) = a_{M,h}^{\text{mixed}}(e_h,w) + r_h(e_h,w) \\
&= a_{M,h}^{\text{mixed}}(e_h, w - v_h) - r_h(u,v_h) + r_h(e_h,w) \\
&= a_{M,h}^{\text{mixed}}(e_h, w - v_h) + r_h(u, w - v_h) - r_h(u,w) + r_h(e_h,w). \qquad (19)
\end{aligned}
$$

Now, from the boundedness of $r_h(\cdot,\cdot)$ in $H^1(\Omega_R)$, lemma 1 and with the use of orthogonal projection $P_h : V \to V_h$ with respect to $H^1(\Omega_R)$-inner product, we have,

$$
\begin{aligned}
|r_h(u,w)| &\le |r_h(u, w - P_h w)| + |r_h(u, P_h w)| \\
&\le C\|u\|_{1,\Omega_R}\|w - P_h w\|_{1,\Omega_R} + C_1(h)\|u\|_{2,\Omega_R}\|P_h w\|_{1,\Omega_R} \\
&\le (Ch + C_1(h))\|u\|_{2,\Omega_R}\|w\|_{2,\Omega_R}, \\
|r_h(e_h,w)| &\le |r_h((I-P_h)e_h, w)| + |r_h(P_h e_h, w)| \\
&\le C\|(I-P_h)u\|_{1,\Omega_R}\|w\|_{1,\Omega_R} + C_1(h)\|e_h\|_{1,\Omega_R}\|w\|_{2,\Omega_R} \\
&\le (Ch\|u\|_{2,\Omega_R} + C_1(h)\|e_h\|_{1,\Omega_R})\|w\|_{2,\Omega_R}.
\end{aligned}
$$

Using $|b_0(e_h, e_h)| = (k^2+1)\|e_h\|^2_{0,\Omega_R}$, the boundedness of $a_M^{\text{mixed}}(\cdot,\cdot)$ and $r_h(\cdot,\cdot)$, the fact that $\inf_{v_h\in V_h}\|w-v_h\|_{1,\Omega_R} \le Ch\|w\|_{2,\Omega_R}$, and (18), we have from (19),

$$\begin{aligned}
(k+1)\|e_h\|^2_{0,\Omega_R} &\le C(\|e_h\|_{1,\Omega_R}+\|u\|_{1,\Omega_R})\inf_{v_h\in V_h}\|w-v_h\| \\
&\quad +\{C_1(h)\|e_h\|_{1,\Omega_R}+(2Ch+C_1(h))\|u\|_{2,\Omega_R}\}\|w\|_{2,\Omega_R} \\
&\le \|e_h\|_{0,\Omega_R}\{C_5(h)\|e_h\|_{1,\Omega_R}+C_6(h)\|u\|_{2,\Omega_R}\} \\
&\le \varepsilon\|e_h\|^2_{0,\Omega_R}+C(\varepsilon)\{C_5^2(h)\|e_h\|^2_{1,\Omega_R}+C_6^2(h)\|u\|^2_{2,\Omega_R}\},
\end{aligned}$$

where $C_5(h) = Ch + C_1(h), C_6(h) = 3Ch + C_1(h)$. Rearranging the inequality completes the proof. □ □

6 Numerical tests and results

We present in this section some of the results of numerical testings of our method for various examples. We compare the efficiency of our mixed type method with the standard FEM.

All computations were carried out on VT-Alpha5, 533Mhz, 512MB RAM with Linux operating system environment with double precision arithmetic using object oriented C++ codes. The iteration scheme in solving the system of linear equations using fictitious domain method, we use the transpose free quasi minimal residual (TFQMR) by Freund [5]. The residual tolerance was set to $\varepsilon = 10^{-6}$.

6.1 Convergence testing

To test the convergence of the computed solutions and compare with the standard FEM solutions as the mesh size decreases, we consider an example of a circular obstacle of radius $r_1 = 1$ with artificial boundary radius $R = 1.3927$. We choose the wave numbers $k = \pi, 2\pi$ and 10π and the incident wave as a plane wave in the x-axis direction $\phi = 0$. For the finite element mesh, we choose orthogonal partition with size (n_r, n_θ) ranging between (2,16)-(2049,32768). For the standard finite element approach, the infinite series in eigenvalues are computed until machine precision is achieved. The resulting separable linear system is solved by using fast direct method with FFT.

The maximum errors $\|u - u_h^{\text{std}}\|_{\infty,\Omega_R}, \|u - u_h^{\text{mixed}}\|_{\infty,\Omega_R}$ against the angular partition size are shown in Fig. 3(a). The maximum error between the two computed solutions $\|u_h^{\text{std}} - u_h^{\text{mixed}}\|_{\infty,\Omega_R}$ is shown in Fig. 3(b) in logarithmic scale. Both solutions converge linearly as well as their difference.

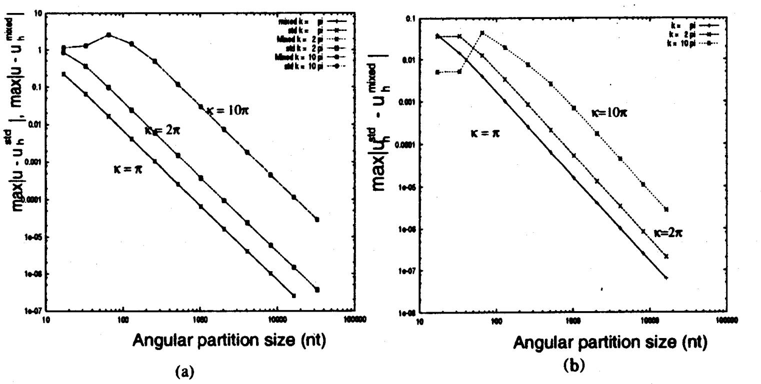

Figure 3: Convergence

6.2 Efficiency testing

To test the computing time difference between the methods, we consider the first test example above and an example with an elliptic shape obstacle with axes $2a = 2.0$ and $2b = 1.2$. The wave number

$k = \pi$. We choose the artificial boundary radius $R = 1.1$ and 3.0. The radial and angular partition sizes $n_r = 40$ and $n_\theta = 256$ respectively. The results are shown in Table 1.

Table 1: Comparison between MTM and standard FEM

R	Obstacle	Std FEM time (sec.)	MTM time (sec.)	Iterations
1.1	Circle	2.42	1.33	11(both)
1.1	Ellipse	5.01	2.74	33 (both)
3.0	Circle	6.41	5.18	11(both)
3.0	Ellipse	14.22	13.51	30 (both)

We also considered an arc shaped obstacle and the Helmholtz resonator with the domain truncated by inner and outer artificial boundaries. The scattering waves and the far-field pattern are computed by using the formula for solution outside the computational domain. From the far-field pattern, the radar cross section (RCS) is computed by using the formula $RCS(\theta) = 10\log_{10}(\omega|F(\theta)|^2)$ which is in decibel units [7]. The total waves (real part) for circular arc with waves number $k = 6\pi$ and scattering waves (real part) for the Helmholtz resonator with wave number $k = 3\pi$ and their radar cross sections are shown in Fig. 4.

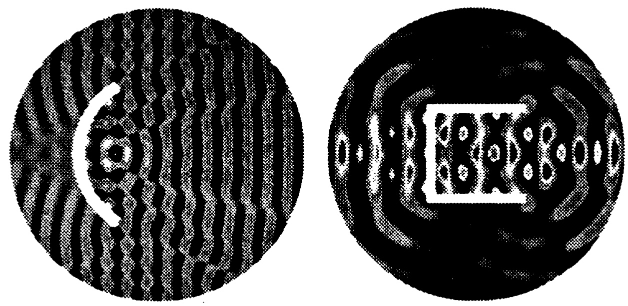

Figure 4: Wave pattern for antenna and Helmholtz resonator

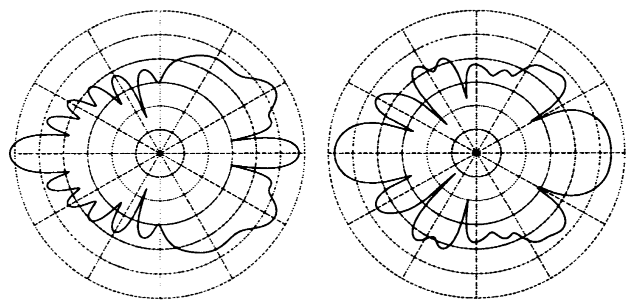

Figure 5: Radar cross sections for antenna and Helmholtz resonator

7 Conclusions

In this paper, we proposed a mixed type method for the finite element approximation of non-local radiation boundary condition written in the form of pseudo-differential operator. We defined a mixed type approximation matrix to approximate the sesqui-linear form corresponding to the DtN operator. The method is also efficiently applied to compute the solution of the radiation problem outside the computational domain and to compute the far-field pattern.

Numerical tests show that the mixed type method is computationally efficient. The convergence is confirmed for the mixed type method and is observed to be of the same order as the standard finite element approximation.

References

[1] Börgers, C., A triangulation algorithm for fast elliptic solvers based on domain imbedding, *SIAM J. Numer. Anal.* **27**, No. 5, (1990) 1187–1196.

[2] Braess, D., *Finite Elements, Theory, Fast Solvers and Applications in Solid Mechanics*, (Cambridge University Press, 1997).

[3] Ciarlet, P. G. and Lions, J. L., *Handbook of Numerical Analysis, Vol II, Finite element methods*, (North Holland, 1991).

[4] Ernst, O. G., A finite-element capacitance matrix method for exterior Helmholtz problems, *Numer. Math.* **75**, No. 2, (1996) 175–204.

[5] Freund, R. W., A Transpose-Free quasi-minimal residual algorithm for non-Hermitian linear systems, *SIAM J. Sci. Comput.* **14**, (1993) 470–482.

[6] Givoli, D., Non-reflecting boundary conditions, *J. Comput. Phys.* **94**, (1991) 1–29.

[7] Heikkola, E., Kusnetsov, Y. A., Neittaanmaki, P. and Toivanen J., Fictitious domain methods for the numerical solution of two-dimensional scattering problems, *J. Comput. Phys.* **145**, (1998) 89–109.

[8] Ihlenburg, F., *Finite Element Analysis of Acoustic Scattering*, Applied Mathematical Sciences, 132 (Springer-Verlag, 1998).

[9] Kako, T., Approximation of scattering state by means of the radiation boundary condition, *Math. Meth. in the Appl. Sci.* **3**, (1981) 506–515.

[10] Keller, J. and Givoli, D., Exact non-reflecting boundary conditions, *J. Comput. Phys.* **94**, (1989) 172–192.

[11] Koyama, D., Mathematical analysis of the DtN finite element method for the exterior Helmholtz problem, Report CS 00-06, Univ. of Electro-Communications, 2000.

[12] Kuznetsov, Yu. A. and Lipnikov, K. N. 3D Helmoltz wave equation by fictitious domain method, *Russ. J. Numer. Anal. Math. Modeling*,**13** No. **5**, (1998) 371–387.

[13] Liu, X., Study on Approximation method for the Helmholtz equation in unbounded region, PhD. thesis, The University of Electro-Communications, Japan, 1999.

[14] Liu, X. and Kako, T., Higher order radiation boundary condition and finite element method for scattering problem, *Advances in Mathematical Sciences and Applications* **8**, No. 2, (1998) 801–819.

[15] Lynch, R. E., Rice, J. R. and Thomas, D., Direct solutions of partial differential equations by tensor product methods, *Numer. Math.* **6** (1964) 185–199.

[16] MacCamy, R. C., Marin, S. P. A, Finite element method for exterior interface problems. *Internat. J. Math. Math. Sci.* **3**, No. 2, (1980) 311–350.

[17] Masmoudi, M., Numerical solution for exterior problems, *Numer. Math.* **51**, (1987) 87–101.

[18] Nirenberg, L., Lectures on linear partial differential equations, *C. B. M. S. Regional Conf. Ser. in Math.*, No. 17, (Amer. math. Soc., Providence, R.I., 1973).

[19] Taylor, M. E., *Pseudo differential Operators*, (Princeton University Press, 1981).

[20] Thompson, I. J. and Barnett, A. R., Coulomb and Bessel functions of complex arguments and order, *J. Comput. Phys.* **64**, (1986) 490–509.